

# Catalysis Science & Technology

Accepted Manuscript



This is an *Accepted Manuscript*, which has been through the Royal Society of Chemistry peer review process and has been accepted for publication.

*Accepted Manuscripts* are published online shortly after acceptance, before technical editing, formatting and proof reading. Using this free service, authors can make their results available to the community, in citable form, before we publish the edited article. We will replace this *Accepted Manuscript* with the edited and formatted *Advance Article* as soon as it is available.

You can find more information about *Accepted Manuscripts* in the [Information for Authors](#).

Please note that technical editing may introduce minor changes to the text and/or graphics, which may alter content. The journal's standard [Terms & Conditions](#) and the [Ethical guidelines](#) still apply. In no event shall the Royal Society of Chemistry be held responsible for any errors or omissions in this *Accepted Manuscript* or any consequences arising from the use of any information it contains.



## Catalysis Science &amp; Technology

## ARTICLE

## Catalytic hydrogenation of liquid alkenes with a silica grafted hydride pincer iridium(III) complex: Support for a heterogeneous mechanism

Received 00th January 20xx,  
Accepted 00th January 20xx

DOI: 10.1039/x0xx00000x

www.rsc.org/

M. Rimoldi,<sup>a†</sup> D. Fodor,<sup>a</sup> J. A. van Bokhoven<sup>a, b</sup> and A. Mezzetti<sup>a\*</sup>

The previously reported silica-grafted iridium(III) hydride complex [IrH(O-SBA-15)(POCOP)] (**2**), prepared by treating [IrH<sub>2</sub>(POCOP)] (**1**) (POCOP is 1,3-bis((di-*tert*-butylphosphino)oxy)benzene) with SBA-15 (mesoporous silica), hydrogenates liquid alkenes (1-decene, *trans*-5-decene, cyclohexene, styrene, and 4-phenyl-1-butene) at room temperature and under 1 atm H<sub>2</sub>. Internal alkenes react at a lower rate than terminal ones. For the sake of comparison, the hydrogenation of the same substrates was studied with the homogeneous catalyst [IrH<sub>2</sub>(POCOP)] (**1**). The heterogeneous catalyst **2** hydrogenates 1-decene, cyclohexene, and 4-phenyl-1-butene faster than **1**, whereas the opposite is true for styrene and *trans*-5-decene, which suggests that different active species are involved in the hetero- and homogeneous reactions. Catalysis by a truly heterogeneous species is supported by a series of “hot filtration tests”. NMR Spectroscopic studies showed that **2** does not undergo degrafting when exposed to alkenes longer than ethene under hydrogenation conditions.

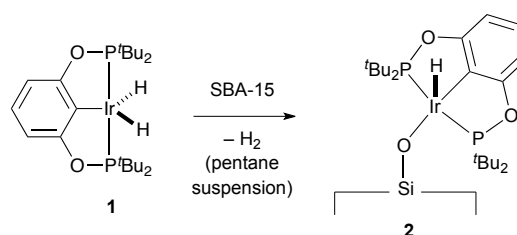
### Introduction

Over the past years, many attempts have been made to combine the selectivity of molecular homogeneous catalysts with the robustness and reusability of heterogeneous systems. Among all, one of the most widespread methods to heterogenise a homogeneous catalyst is to immobilise it onto a surface, generally an inorganic oxide.<sup>1-2</sup> The covalent attachment to the surface is achieved either via anchoring, in which the ligand backbone of the complex is linked to the surface, or via grafting, which involves the formation of a bond between the metal and a surface oxygen.<sup>3-4</sup> The advantage of grafting is that no ligand functionalisation is needed to heterogenise the soluble catalysts.

Oxide-supported, grafted complexes of early transition metals (TMs)<sup>5-7</sup> have been successfully developed and have found application in various catalytic transformations.<sup>8-15</sup> Earlier examples are zirconium and titanium alkyl complexes grafted on silica, whose reaction with dihydrogen gives polyhydride species that are active in alkene polymerisation and alkene hydrogenation under mild conditions.<sup>16-20</sup> Concomitantly,

Marks explored the grafting of the bis(cyclopentadienyl) complexes of actinides [M(CH<sub>3</sub>)<sub>2</sub>(C<sub>5</sub>Me<sub>5</sub>)<sub>2</sub>] (M = Th, U) on alumina,<sup>21-24</sup> which gave a material that is highly active in the hydrogenation of alkenes.<sup>25-26</sup>

At difference with early TMs, late ones have been investigated to a lesser extent in the preparation and characterisation of well-defined species featuring a metal–OSi bond.<sup>27-33</sup> A specific difference from early TMs is that oxide-grafted hydrides of late TMs are unstable and tend to aggregate into metal(0) nanoparticles.<sup>3,34-35</sup> We have recently reported that the dihydride pincer complex [IrH<sub>2</sub>(POCOP)] (**1**) reacts with SBA-15 to give the silica-grafted iridium(III) hydride [IrH(O-SBA-15)(POCOP)] (**2**) (POCOP is the pincer ligand 1,3-bis(di-*tert*-butylphosphino)phenyl) (Scheme 1).



Scheme 1. Synthesis of **2** from [IrH<sub>2</sub>(POCOP)] (**1**).

This compound, which is a rare example of a well-defined and stable hydride complex of a late TM grafted on an oxide surface, catalyses the hydrogenation of gaseous alkenes (ethene and propene) at a total pressure of 2 bar abs.<sup>36</sup> At room temperature, TOFs of 7.3 and 5.3 min<sup>-1</sup> were achieved for ethene respectively propene, whereas the reaction at 70°C

<sup>a</sup> Department of Chemistry and Applied Biosciences, ETH Zürich  
Vladimir-Prelog-Weg 2, CH-8093, Switzerland.  
E-mail: mezzetti@inorg.chem.ethz.ch

<sup>b</sup> Laboratory for Catalysis and Sustainable Chemistry, Paul Scherrer Institute, 5335  
PSI Villigen, Switzerland.

† Present address: Department of Chemistry, Northwestern University, 2145  
Sheridan Road, Evanston, Illinois 60208, USA.

Electronic Supplementary Information (ESI) available: additional experimental  
details, NMR spectra and crystallographic data for **6a** and **6b**. See  
DOI: 10.1039/x0xx00000x

## ARTICLE

## Catalysis Science &amp; Technology

gave TOFs of 28.7 and 24.7  $\text{min}^{-1}$ . Interestingly, the catalyst was active without any chemical or thermal activation, was recovered without sign of decomposition after catalysis, and was reused without loss of activity.

Some of us have recently reported that **2** and its soluble analogues [IrH(*i*Bu-POSS)(POCOP)] (**3**) (*i*Bu-POSS is isobutyl-substituted polysilsesquioxane,  $-\text{OSi}_8\text{O}_{12}/\text{Bu}_7$ ) and [IrH(OSiMe<sub>3</sub>)(POCOP)] (**4**) (Fig. 1) react with carbon monoxide to give the corresponding six-coordinate adducts, which then undergo reductive elimination of silanol and release the degrafted iridium(I) complex [Ir(CO)(POCOP)].<sup>37</sup>

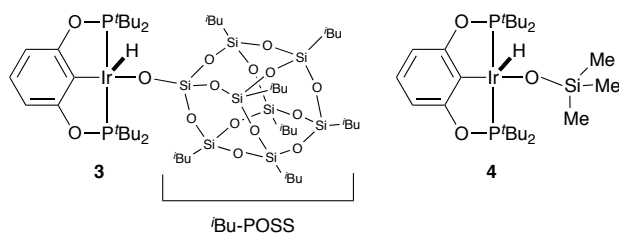


Fig. 1. Soluble siloxo derivatives **3** and **4**.

The reductive elimination of silanol is a major potential problem that faces the application of such grafted complexes in the hydrogenation of liquid olefins. The present work addresses the issue of degrafting during the catalytic hydrogenation of liquid alkenes, such as 1- and *trans*-5-decene, cyclohexene, styrene, and 4-phenyl-1-butene, for all of which leaching tests were carried out. Furthermore, we report the stoichiometric reactions of **2** and of its homogeneous analogues **3** and **4** with representative liquid alkenes, dihydrogen, and as well as in the presence of an alkene-dihydrogen mixture.

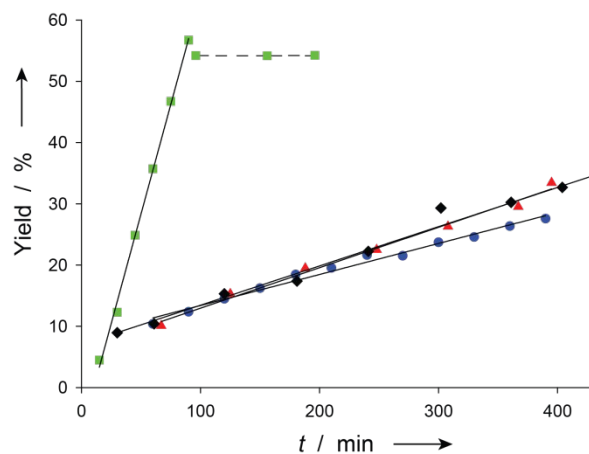
## Results and Discussion

### Hydrogenation of 1-decene

For the sake of comparison with the hydrogenation of ethene and propene,<sup>36</sup> a linear terminal alkene such as 1-decene was studied first with [IrH(O-SBA-15)(POCOP)] (**2**), the dihydride complex [IrH<sub>2</sub>(POCOP)] (**1**), and the soluble analogue [IrH(*i*Bu-POSS)(POCOP)] (**3**)<sup>37</sup> as catalysts in pentane solution. To enable comparison between data obtained from catalytic runs under homogeneous respectively heterogeneous conditions, the same amounts of pincer complex and substrate were used in all reaction. The dihydrogen pressure was kept constant at 1 bar (abs.) in all reactions and over the entire reaction time, which allowed a periodic sampling of the reaction mixture. The reaction profiles are shown in Fig. 2. The rate is approximately constant over the conversion range studied and gives the TOF value (Fig. S1) reported in Table 1.

The silica-grafted complex [IrH(O-SBA-15)(POCOP)] (**2**) catalysed the hydrogenation of 1-decene with a TOF of 8.4  $\text{h}^{-1}$ , whereas the reaction with dihydride **1** was significantly slower (TOF = 0.72  $\text{h}^{-1}$ ).<sup>‡</sup> As the TOF observed for the silica-grafted catalyst **2** exceeds by 11.5 times that obtained with the maximum concentration of **1** that can be obtained upon

complete leaching of the iridium complex, we rule out that the active species is a portion of the grafted catalyst **2** that has been released as **1** in solution during catalysis.



- (a) [IrH(SBA-15)(POCOP)] (**2**)
- (b) [IrH<sub>2</sub>(POCOP)] (**1**)
- ▲ (c) [IrH(POSS)(POCOP)] (**3**)
- ◆ (d) [IrH(SBA-15)(POCOP)] (**3**) + excess of POSS

Fig. 2. Hydrogenation of 1-decene with **2** and its homogeneous analogues **1** and **3**.

Table 1. TOF values ( $\text{h}^{-1}$ ).<sup>[a],[b]</sup>

Substrate	[IrH(O-SBA-15)(POCOP)] ( <b>2</b> )	[IrH <sub>2</sub> (POCOP)] ( <b>1</b> )
Ethene <sup>[c]</sup>	438 <sup>[d]</sup>	-
Propene <sup>[c]</sup>	306 <sup>[e]</sup>	-
1-Decene	8.4	0.72 <sup>[f]</sup>
Trans-5-Decene	0.42	0.70
Cyclohexene	1.4	1.1
Styrene	2.6	18.3 <sup>[f]</sup>
4-Phenyl-1-butene	3.8	1.1 <sup>[f]</sup>

<sup>[a]</sup> Calculated from Fig. S1, S3, S7-S10, and S12-S15. <sup>[b]</sup> Reaction conditions: Pincer complex: 5 mg, 4.2 mol% catalyst loading, substrate: approximately 200  $\mu\text{mol}$ , solvent: pentane (5 mL), dihydrogen: 1 bar abs. <sup>[c]</sup> From ref. 36. <sup>[d]</sup> Determined after 30 min and at 20% ethene conversion. <sup>[e]</sup> Determined after 30 min and at 14% propene conversion. <sup>[f]</sup> The virtually instantaneous alkene conversion observed at time zero (Y intercept) was not considered to calculate TOF ( $\text{h}^{-1}$ ) values.

To double-check the absence of leaching, a “hot filtration test” was performed. The hydrogenation reaction was run for 90 min up to a conversion of 56.7%, and then the stirring was interrupted. After the heterogeneous catalyst had deposited, which occurred within a few seconds, most of the colourless supernatant solution was transferred by syringe into a new reaction vessel under dihydrogen (1 bar abs.) to preserve the catalysis conditions. The monitoring of the reaction in this portion of the solution during 1.5 h showed that 1-decene was not being hydrogenated further (Fig. 2, dashed line), which confirms that the active catalyst is a silica-bound complex and not a species released into the solution.

After the catalytic run, the solid catalyst was separated from the liquid phase by filtration, and its solid-state <sup>31</sup>P NMR spectrum was measured and found to be identical to that of an

unused sample of **2** (Fig. 3). Consistently with this finding, a recycling test of the solid catalyst showed only minimal differences between the first and the second run (Fig. 4).

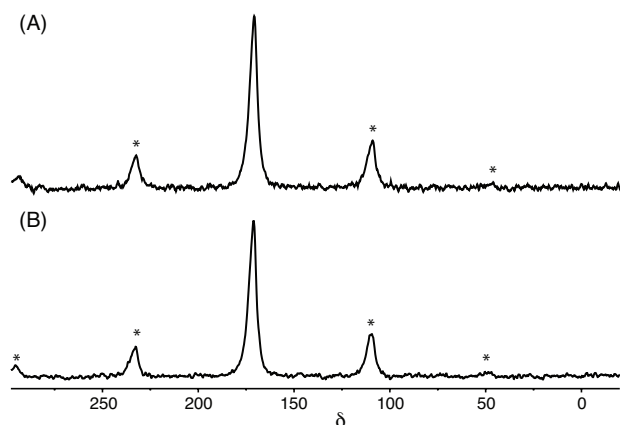


Fig. 3.  ${}^1\text{H}$ - ${}^{31}\text{P}$  MAS NMR spectrum of catalyst **2** before (A) and after (B) 1-decene hydrogenation ("\*" denotes spinning side bands).

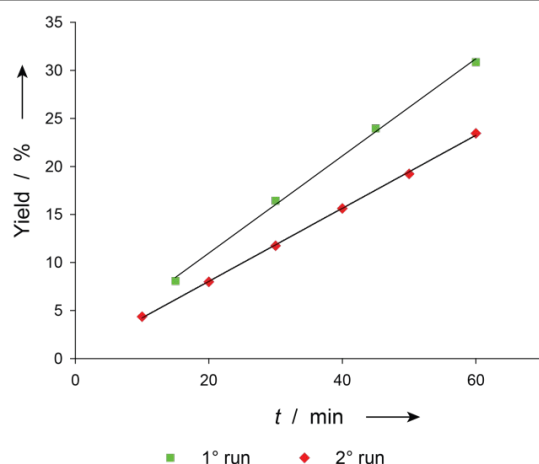


Fig. 4. Recycling of the catalyst **2** in the hydrogenation of 1-decene

As POSS complexes are generally used as homogeneous analogues of silica-grafted complexes, we tested the POSS derivative  $[\text{IrH}(\textit{i}\text{Bu-POSS})(\text{POCOP})]$  (**3**) in the hydrogenation of 1-decene for the sake of comparison. The reaction profile with **3** is essentially indistinguishable from that of the catalytic reaction with dihydride **1** (Fig. 2 *b, c*, and S4, S5).

In fact, the pentane solution of **3** turned from red to light yellow when put under dihydrogen (1 atm), which indicates the formation of the tetrahydride  $[\text{IrH}_4(\text{POCOP})]$  (**5**) (see Scheme 8 below). This suggests that the exposure of **3** to dihydrogen produces free silanol and dihydride **1** to eventually form the tetrahydride complex **5**, as independently indicated by the stoichiometric reaction of **3** with dihydrogen (see below).

Upon addition of 1-decene, the solution turned red as the corresponding alkene complex  $[\text{Ir}(1\text{-decene})(\text{POCOP})]$  (**6c**) was formed,<sup>‡</sup> as confirmed by  ${}^{31}\text{P}$  NMR spectroscopy. As the catalytic behaviour of **1** and **3** is essentially identical (Fig. 2), only dihydride **1** was used with the other substrates. Therefore, the POSS derivative **3** was not investigated further.

Finally, to simulate the excess of free silanols present in the reaction catalysed by the silica-grafted complex **2**, a 10-fold excess of POSS was added to the POSS complex **3**, which gave similar results in the hydrogenation of 1-decene (Fig. 2 *d*) and the same visual changes of the colour of the reaction solution. The comparison of Fig. 2 *b–d* shows no significant differences between the homogeneous reactions with the soluble complexes **1** and **3** under different conditions, which suggests that they are all catalysed by the same species. Besides activity, a further difference between the silica-grafted catalyst **2** and its homogeneous analogues **1** and **3** was observed that concerns the isomerisation of 1-decene to internal alkenes (see below).

### Isomerisation of 1-decene

The GC-MS analysis of the products of hydrogenation of 1-decene catalysed by the grafted complex **2** showed that three isomers of 1-decene are formed in small, but detectable amounts during the reaction. The total yield of these isomers reaches approximately 5% at about 57% yield of decane, and the isomerisation stops upon removal of the solid catalyst (Fig. S4), which is consistent with the lack of leaching described above.

When monitored to completeness, the concentration of the isomerised products declined after the yield of decane had reached ca. 85% (Fig. S5 and S6). At difference with the silica-grafted catalyst **2**, no internal alkenes were detected with the soluble complexes  $[\text{IrH}_2(\text{POCOP})]$  (**1**) and  $[\text{IrH}(\textit{i}\text{Bu-POSS})(\text{POCOP})]$  (**3**), although dihydride **1** is known to isomerise terminal alkenes at room temperature.<sup>38</sup> The different isomerisation behaviour of the silica catalyst **2** as compared to **1** and **3** further supports a different hydrogenation mechanism for the heterogeneous and soluble catalysts.<sup>5</sup>

### Hydrogenation of internal alkenes

To understand the different isomerisation behaviour of the grafted and soluble catalysts, *trans*-5-decene was hydrogenated with **1** and **2** under the same conditions used for 1-decene (Fig. 5a). The TOF values in Table 1 show that the grafted complex **2** hydrogenates *trans*-5-decene at a much slower rate than 1-decene, whereas the homogeneous catalyst **1** gives the same rate with both isomers. Therefore, the accumulation of internal isomers is possible during the hydrogenation of 1-decene with **2**, but not with **1**. Also with 5-decene, a hot filtration tests indicated that the solution is not catalytically active.

Cyclohexene, which was tested as a model for *cis* internal alkenes, was hydrogenated by the grafted catalyst **2** about three times faster than *trans*-5-decene (Table 1). With TOFs of  $1.1 \text{ h}^{-1}$  and  $1.4 \text{ h}^{-1}$ , respectively, the activity of the soluble dihydride **1** is comparable to that of **2** (Fig. 5b). Also, the phase separation test showed that there is no leaching into solution, in agreement with the findings described above for 1-decene and *trans*-5-decene.

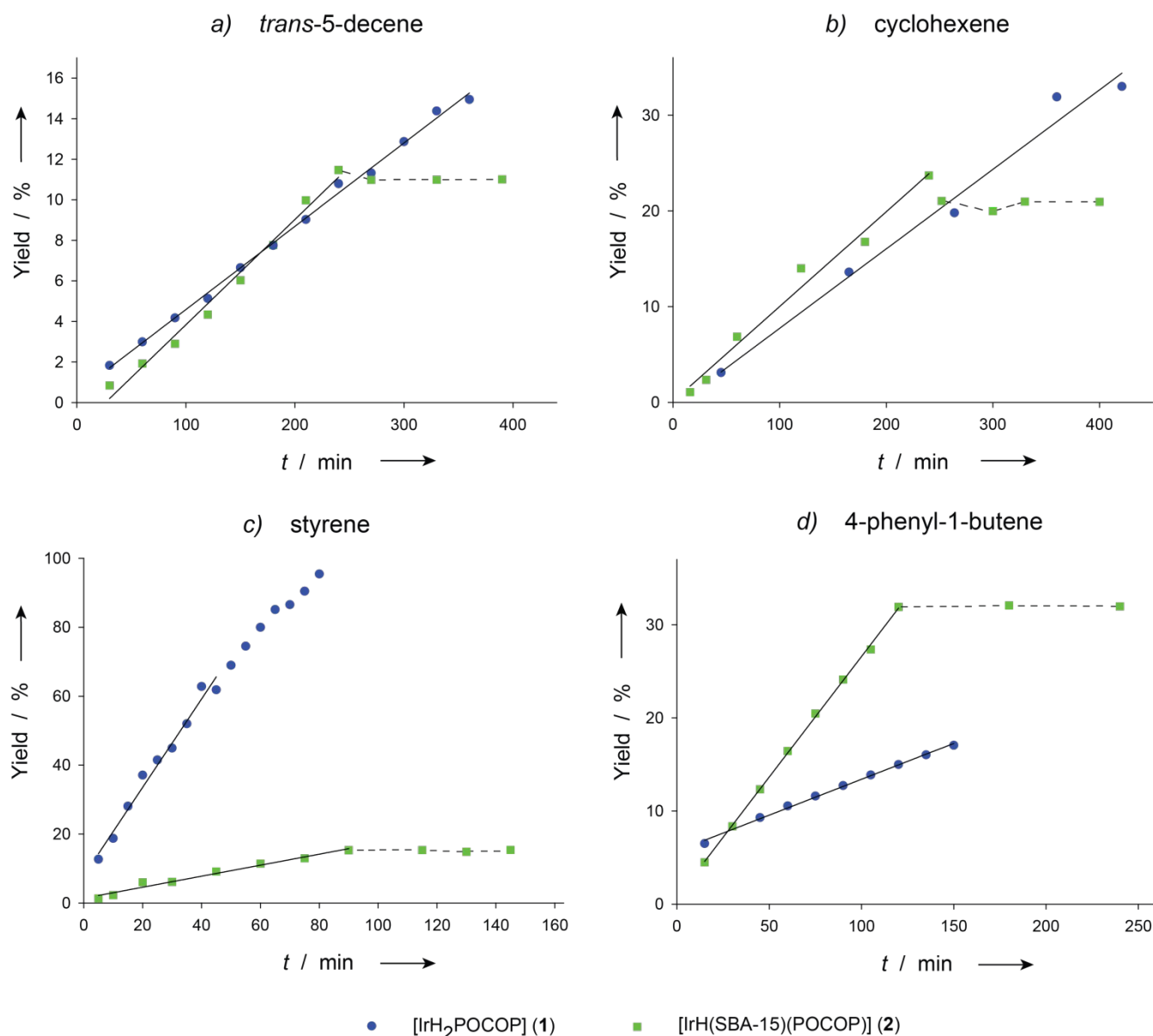


Fig. 5. Hydrogenation of alkenes with **1** and **2** (dashed line refers to "hot filtration tests").

### Styrene and 4-phenyl-1-butene

Finally, the effect of aromatic substituents was studied. At difference with the other substrates tested, styrene was hydrogenated at a significantly higher rate by the homogeneous catalyst **1** than by the silica-grafted **2** (TOF was 18.3 vs. 2.6  $\text{h}^{-1}$ ) (Fig. 5c). Again, **2** did not leach into the reaction solution, as indicated by the filtration test (dashed line in Fig. 5c). The GC-MS analysis of the reaction products showed that both the hetero- (**2**) and the homogeneous (**1**) catalysts gave ethyl benzene as the only detectable product. No species deriving from the hydrogenation on the aromatic ring were observed, which may have suggested the formation of metal nanoparticles that are known to catalyse the

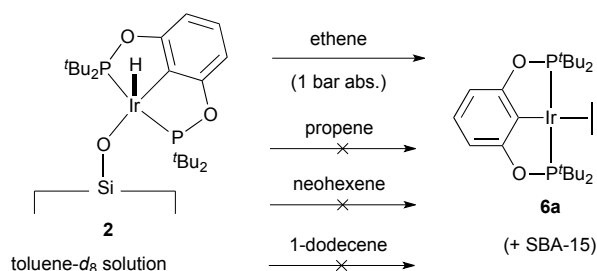
hydrogenation of aromatics under mild conditions in the case of rhodium, iridium, and Pd/Pt.<sup>34,39-40</sup>

At difference with styrene, 4-phenyl-1-butene was hydrogenated at higher rate by the silica-grafted catalyst **2** than by the soluble dihydride **1** (TOF was 3.8  $\text{h}^{-1}$  vs. 1.1  $\text{h}^{-1}$ ) (Fig. 5d), as observed for the other aliphatic alkenes discussed above. As for 1-decene, also the hydrogenation of 4-phenyl-1-butene was accompanied by the formation of products of the double bond isomerisation. With the silica-grafted complex **2**, the total amount of internal isomers was approximately 1.5% (at 31.9% of 4-phenylbutane yield (Fig. S11), whereas the homogeneous catalyst **1** gave a roughly stationary isomer concentration (0.2%).

## Stoichiometric reaction of 2-4 with alkenes

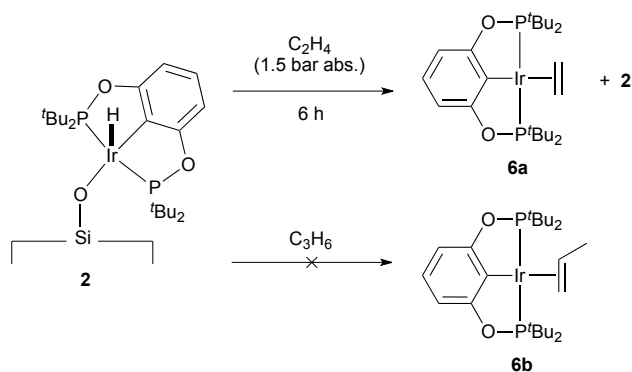
Complexes of the type  $[\text{IrH}_2(\text{pincer})]$  and  $[\text{Ir}(\text{C}_2\text{H}_4)(\text{pincer})]$  with aryl-substituted POCOP ligands have been recently reported to catalyse the hydrogenation of gaseous alkenes.<sup>41</sup> Thus, in the case of **2**, one might speculate that the competent catalyst is a physisorbed, non-chemically bound species formed upon degrafting of **2** under hydrogenation conditions rather than a silica-grafted species. Therefore, we studied the reaction of **2** and of its soluble analogues with ethene, propene, 1-dodecene, and neohexene.

The silica-grafted complex **2** was suspended in  $[\text{D}_8]$ toluene in a gas-tight NMR tube and the liquid alkenes (1-dodecene or neohexene, approx. 20  $\mu\text{L}$ ) were added. For ethene and propene, the solvent was saturated with the gaseous alkene. The  $^1\text{H}$  and  $^{31}\text{P}$  NMR spectra of the liquid phase showed that, with propene, 1-dodecene, and neohexene, no iridium(I) complex was released into the solution, whereas the signals of the iridium(I) ethene complex  $[\text{Ir}(\text{C}_2\text{H}_4)(\text{POCOP})]$  (**6a**) were detected a few minutes after the addition of ethene (1 bar) to the suspension of the grafted complex **2** (Scheme 2).



Scheme 2. Reactivity of **2** in solution with liquid and gaseous alkenes.

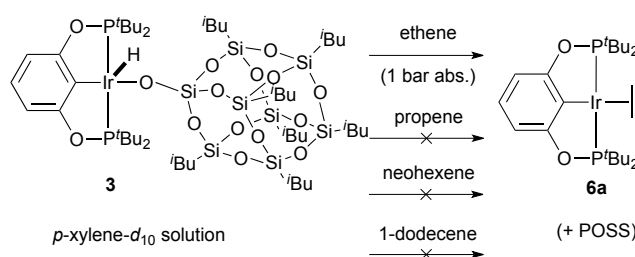
To double-check that only ethene triggers the reductive elimination of silanol from the silica grafted complex **2**, the reactions were repeated with gaseous ethene and propene. When a sample of the silica-grafted hydride **2** was exposed to an ethene atmosphere (1.5 bar) for 6 h at room temperature, a new signal at  $\delta$  182 appeared in the solid-state  $^{31}\text{P}$  NMR spectrum of the recovered sample, which indicates the formation of the iridium(I) ethene complex  $[\text{Ir}(\text{C}_2\text{H}_4)(\text{POCOP})]$  (**6a**) by reductive elimination of silanol (Scheme 3 and Fig. S17).<sup>42</sup>



Scheme 3. Reactivity of **2** in gas-phase with ethene and propene.

The residual signal of the starting material **2** indicates that the conversion to **6a** is not quantitative. However, when propene was used instead of ethene under otherwise same conditions, no reaction was observed, and the solid-state  $^{31}\text{P}$  NMR spectrum showed only the signal of the starting material **2**.

The reactions with alkenes were studied also with the siloxo complexes  $[\text{IrH}(\text{OSi}_8\text{O}_{12}/i\text{Bu}_7)](\text{POCOP})$  (**3**) and  $[\text{IrH}(\text{OSiMe}_3)(\text{POCOP})]$  (**4**), the soluble analogues of **2**. When a  $[\text{D}_{10}]p$ -xylene solution of the POSS complex **3** was saturated with ethene (1 bar absolute), the conversion to the iridium(I) complex  $[\text{Ir}(\text{C}_2\text{H}_4)(\text{POCOP})]$  (**6a**) was almost quantitative within 30 h, as indicated by the signal at  $\delta$  180.6 in the  $^{31}\text{P}$  NMR spectra of the reaction solution (Scheme 4, see Fig. S18).



Scheme 4. Reactivity of **3** with liquid and gaseous alkenes.

Analogously to the silica-grafted complex **2**, the POSS derivative **3** failed to react with propene or with the longer terminal alkene 1-dodecene (Scheme 4). The trimethylsiloxo complex **4** reacted with ethene in  $p$ -xylene solution much faster than POSS derivative **3** to give the reductive elimination product **6a** quantitatively. Upon standing, the ethene complex **6a** crystallised out, and a single crystal X-ray analysis confirmed its identity (Fig. 6). For the sake of comparison, the propene analogue  $[\text{Ir}(\text{C}_3\text{H}_6)(\text{POCOP})]$  (**6b**) was prepared (see Supporting Information),<sup>38</sup> and its X-ray structure was determined.<sup>41</sup>

The reactivity described above clearly shows that ethene behaves differently from higher alkene, including propene, whose reactivity is analogous to that of the liquid alkenes. The X-ray structures of **6a** and **6b** (Fig. 6) give some insight into the different tendency of ethene and propene to induce the reductive elimination from the siloxo complexes **2** and **3**.

In both alkene complexes **6a** and **6b**, the C=C double bond is rotated out of the plane of the complex as usually observed in square-planar complexes. The alkene ligand and two *tert*-butyl groups of the propene derivative **6b** are affected by disorder (not shown in Fig. 6, see Fig. S19), which hinders the structural comparison with **6a**. However, the iridium–alkene distances are appreciably longer in the propene complex **6b** (2.20 and 2.21 Å for Ir–C(23) and Ir–C(24), respectively) than in the ethene analogue **6a** (2.178(3) and 2.185(3) Å). We conclude that the propene complex **6b** is more crowded than the ethene analogue **6a**. Therefore, the failure of the bulky SBA-15 (**2**) and POSS (**3**) derivatives to react with higher alkenes can be attributed to steric effects. This is further supported by the sluggish reaction of the POSS derivative **3** with ethene as compared to the trimethylsiloxo derivative **4**, which reacts much faster (see above).

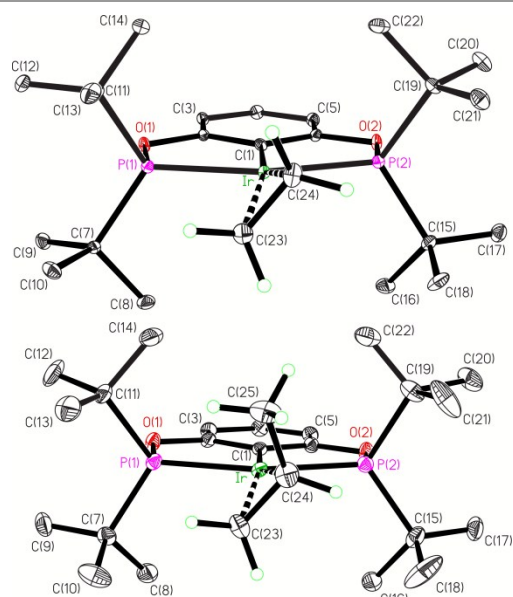
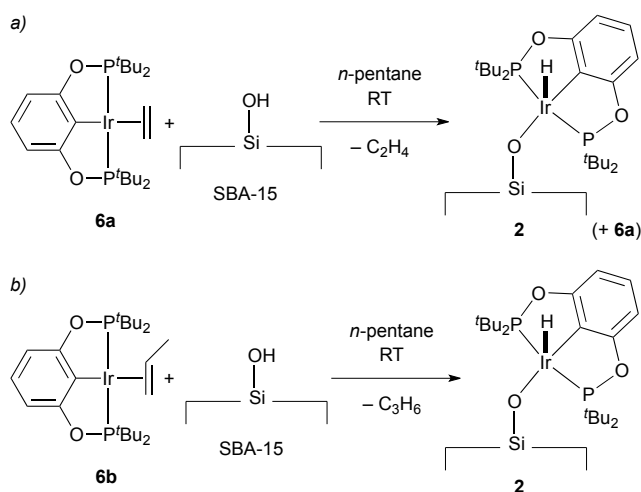


**Fig. 6.** ORTEP diagrams of the alkene complexes **6a** (ethene, top) and **6b** (propene, bottom) (30% probability ellipsoids). Only one set of the disordered propene and *tert*-butyls is shown. Hydrogen atoms, except those of the alkene ligands, are omitted for clarity.

Overall, these results suggest that, compared to its ethene analogue **6a**, the propene complex **6b** is not stable enough to trigger the reductive elimination of silanol. Interestingly, it has been reported previously that the anilido complexes  $[\text{IrH}(\text{NHAr})(\text{POCOP})]$  react with ethene to give aniline and the reductive elimination product **6a**,<sup>43</sup> but we are not aware of analogous reactions with higher alkenes. The implications of these observations for catalysis will be discussed below.

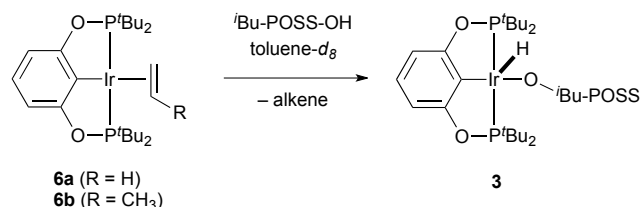
#### Reaction of **6a** and **6b** with silanols

To assess the relative stability of the siloxo hydride complexes of iridium(III) as compared to the corresponding Ir(I) alkene derivatives, the inverse reactions were studied by treating the alkene complexes  $[\text{Ir}(\text{C}_2\text{H}_4)(\text{POCOP})]$  (**6a**) and  $[\text{Ir}(\text{C}_3\text{H}_6)(\text{POCOP})]$  (**6b**) with SBA-15 and *i*Bu-POSS. When SBA-15 was added to a pentane solution of **6a** or **6b** (Scheme 5) under identical experimental conditions, the colour of the solution decreased in intensity over time, and the SBA-15 turned from white to orange. In both reactions, the solid recovered by removing the solvent in vacuum was the silica-grafted species  $[\text{IrH}(\text{O}-\text{SBA-15})(\text{POCOP})]$  (**2**) as indicated by <sup>31</sup>P MAS NMR spectroscopy.<sup>36</sup> However, the solution became completely colourless with the propene complex **6b**, whereas the ethene analogue **6a** did not react quantitatively. Accordingly, the <sup>31</sup>P solid-state NMR spectrum (Fig. S20) of reaction *a* in Scheme 5 showed the presence of unreacted ethene complex **6a**, in agreement with the colour changes of the reaction solution described above. This behaviour confirms that the ethene complex **6a** is more stable than its propene analogue **6b**. It should be noted that the reaction of an iridium(I) alkene complex and surface silanols represents an alternative synthetic pathway to **2**, which has been originally prepared by treating dihydride  $[\text{IrH}_2(\text{POCOP})]$  with SBA-15.<sup>36</sup>



**Scheme 5.** Reactivity of **6a** and **6b** with SBA-15.

The reactivity of the alkene complexes **6a** and **6b** with POSS in  $[\text{D}_8]$ toluene (Scheme 6) parallels that with SBA-15. The ethene complex **6a** did not react with the homogeneous POSS silanol at room temperature, whereas the propene derivative **6b** gave 22% conversion to  $[\text{IrH}(\textit{i}\text{Bu-POSS})(\text{POCOP})]$  (**3**) after 10 min of reaction time, as determined by <sup>1</sup>H and <sup>31</sup>P NMR spectroscopy. However, the equilibrium can be shifted toward the siloxo complexes by heating the reaction solution at 80 °C under static vacuum. Under these conditions, the ethene complex **6a** reacted with POSS to give **3** in 29% yield after 12 h, whereas the propene complex **6b** formed the five-coordinate POSS-hydride iridium complex **3** quantitatively. These observations conclusively support the lower stability of the propene complex **6b** as compared to the ethene analogue **6a**.

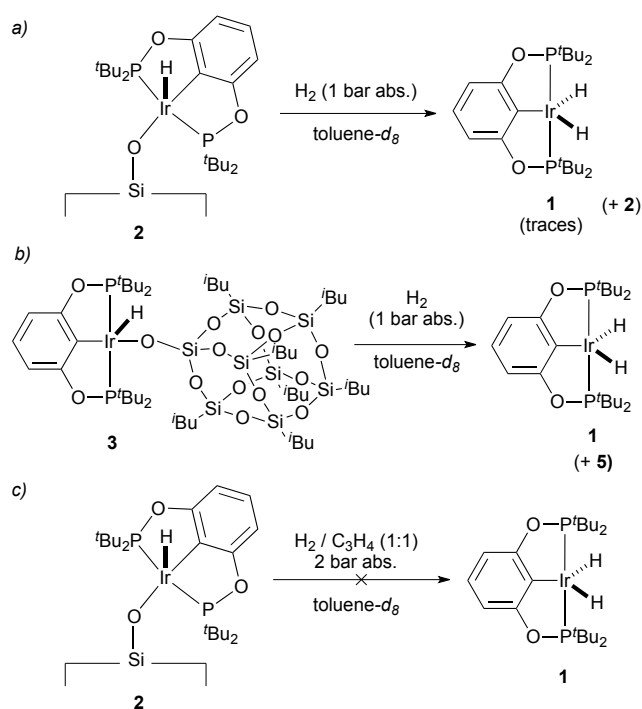


**Scheme 6.** Reactivity of **6a** and **6b** with *i*Bu-POSS.

#### Reaction of **2** and **3** with dihydrogen

Beside alkenes, dihydrogen might trigger the degrafting of the silica-grafted pincer complex  $[\text{IrH}(\text{O}-\text{SBA-15})(\text{POCOP})]$  (**2**) (Scheme 7a). In a preliminary study, a  $[\text{D}_8]$ toluene solution of the POSS analogue **3** was exposed to dihydrogen (1 bar), which resulted in the formation of a mixture of  $[\text{IrH}_2(\text{POCOP})]$  (**1**) and of the corresponding tetrahydride complex  $[\text{IrH}_4(\text{POCOP})]$  (**5**), as determined by <sup>31</sup>P and <sup>1</sup>H NMR spectroscopy (Scheme 7b). In contrast, when the silica-grafted complex  $[\text{IrH}(\text{O}-\text{SBA-15})(\text{POCOP})]$  (**2**) was suspended in  $[\text{D}_8]$ toluene in an NMR tube under dihydrogen (1 bar), the <sup>1</sup>H NMR spectrum of the reaction solution showed a small signal at  $\delta -8.4$  in the hydride region, which indicates that only trace amounts (approximately 4% by <sup>1</sup>H NMR spectroscopy) of the grafted complex **2** are released into solution as the tetrahydride complex **5** under

such conditions. Reaction monitoring by  $^1\text{H}$  NMR spectroscopy indicates that the traces of tetrahydride complex **5** are formed instantaneously upon addition of hydrogen and no progress of the reaction are observed over 30 min.



Scheme 7. Reactivity of siloxo species with dihydrogen.

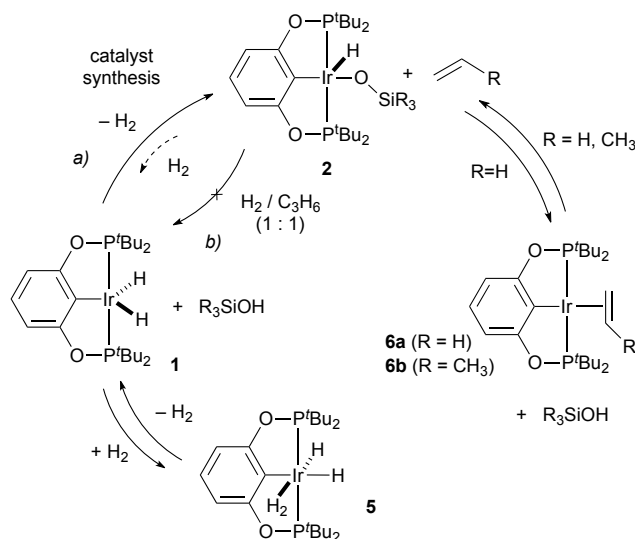
Interestingly, however, when a suspension of the silica-grafted hydride **2** was exposed to a gaseous mixture of hydrogen and propene (1:1), neither dihydride **1** nor tetrahydride **5** were detected in solution by NMR spectroscopy after 45 min (Scheme 7c). The lack of detectable degrafting under a dihydrogen/propene atmosphere is in agreement with the results of the hot filtration tests for liquid alkenes described above.

#### Stoichiometric reaction: Relevance to catalysis

The stoichiometric reactions summed up in Scheme 8 reveal a number of intriguing features that can explain the lack of degrafting observed in catalysis. The reactions with alkenes show that, although both the ethene complex  $[\text{Ir}(\text{C}_2\text{H}_4)(\text{POCOP})]$  (**6a**) and its propene analogue **6b** oxidatively add silanol to give the grafted complex **2**, only ethene triggers the inverse reaction, that is, the reductive elimination of silanol from **2** that releases **6a** in solution. The X-ray structures of the ethene (**6a**) and propene (**6b**) derivatives suggest that the iridium(I) complexes  $[\text{Ir}(\text{alkene})(\text{POCOP})]$  with higher alkenes are too crowded to be stable with respect to the grafted hydride **2**. We conclude that higher alkenes cannot induce reductive elimination of silanol and thus degrafting.

Under hydrogenation conditions, however, the reaction with  $\text{H}_2$  offers an alternative possibility for degrafting. Concerning this issue, it is of particular importance that the silica-grafted siloxo complex **2** barely reacts with dihydrogen to eliminate silanol, as mentioned above. In fact, the NMR spectroscopic

monitoring of the reaction of **2** with dihydrogen (1 atm) (see above) shows that only a small amount (4 %) of **2** undergoes rapid degrafting and that the concentration of the degrafted species does not increase with time. These observations indicate that the equilibrium *a*) in Scheme 8 is rapidly established and that the grafted complex **2** is thermodynamically favored as compared to **1** (at least under 1 atm  $\text{H}_2$ ).



Scheme 8. Reactivity overview.

In contrast, the iridium(III) POSS complex **3** gives mainly dihydride **1**, tetrahydride **5**, and silanol when exposed to dihydrogen (1 atm), which can be explained with subtle differences in the overall donor ability of *i*Bu-POSS and SBA-15.<sup>37</sup> We conclude that **2** is more stable than its soluble siloxo analogues **3** and **4** toward silanol elimination under  $\text{H}_2$  under the experimental conditions used.

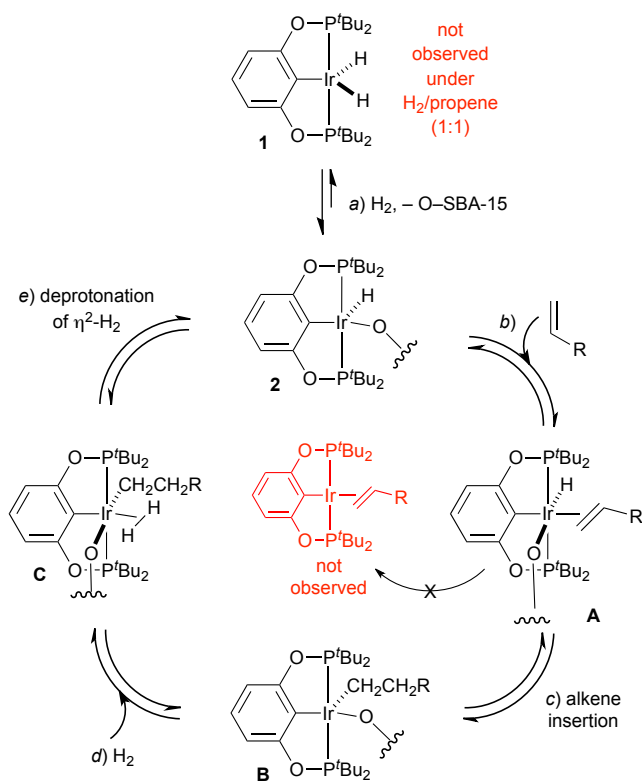
Even more importantly, the formation of  $[\text{IrH}_4(\text{POCOP})]$  (**5**) (or of  $[\text{IrH}_2(\text{POCOP})]$  (**1**)) is completely suppressed in the presence of  $\text{H}_2$  and propene, that is, under hydrogenation conditions (Scheme 8b). This is a very important observation, because, in the hydrogenation catalysed by the soluble dihydride  $[\text{IrH}_2(\text{POCOP})]$  (**1**), the iridium(I) alkene complex  $[\text{Ir}(\text{alkene})(\text{POCOP})]$  is the resting species of the hydrogenation of alkenes.<sup>11</sup> Hence, its signals should be observable in the  $^1\text{H}$  and  $^{31}\text{P}$  NMR spectra of the reaction solution of the hydrogenation catalysed by the grafted complex **2** if leaching would occur during catalysis, which is not the case.

#### Mechanism of catalysis: A working hypothesis

Although a mechanistic study is beyond the scope of this paper, the experimental observations in the catalytic and stoichiometric reactions reported above are completely compatible with the working hypothesis for the reaction pathway that we reported previously<sup>36</sup> (Scheme 9). In particular, it offers an explanation for the lack of degrafting of **2** during the hydrogenation of liquid olefins, which is the most striking feature of the present study. The direct involvement of the 16-electron, silica-grafted monohydride complex **2** in the

catalytic cycle is corroborated by the fact that it is active without previous activation, is isolated unchanged after catalysis, and is equally active when reused. This conclusion is of paramount importance, as it implies a monohydride mechanism in which the silica-grafted complex **2** is the active species.

Then, the observation that propene suppresses the elimination of silanol from **2** under  $H_2$  suggests that the insertion of the alkene into the Ir–H bond of **2** (Scheme 9b and c) is faster than the  $H_2$ -induced elimination of silanol (Scheme 9a). Furthermore, the latter reaction is also thermodynamically disfavored at  $P(H_2) = 1$  atm, as indicated by the corresponding stoichiometric reaction, in which only a small amount of dihydride **1** is released in solution (see above). Also, both the failure of **2** to react with higher alkenes and the absence of [Ir(alkene)(POCOP)] in solution during catalysis suggest that intermediate **A** undergoes alkene insertion faster than reductive elimination of silanol to give the corresponding alkene complex [Ir(alkene)(POCOP)] (in red in Scheme 9).



Scheme 9. Mechanistic working hypothesis.

There is barely literature precedent of iridium-catalysed hydrogenation reactions based on monohydride complexes, and the alternative dihydride pathway that involves oxidative addition of  $H_2$ , alkene insertion into the M–H-bond, and reductive elimination of the alkane is nearly ubiquitous. A possible monohydride pathway might encompass alkene insertion into the Ir–H bond of a monohydride complex (b and c), followed by  $H_2$  coordination onto the resulting iridium(III) alkyl complex **B** (d). Finally, the intramolecular deprotonation of the  $\eta^2-H_2$  ligand by the alkyl ligand in **C** might form the alkane and regenerate the monohydride iridium(III) complex **2** according

to e). Interestingly, the latter step has been calculated to be the lowest-energy pathway for the asymmetric hydrogenation reactions of alkenes catalysed by  $[IrH_2(H_2)(C_2H_4)(C-N)]^+$  (C–N is a carbene oxazoline ligand).<sup>44</sup>

The fact that the monohydride complex [IrH(O–SBA-15)(POCOP)] (**2**) is the active species in catalysis implies that the mechanism of the heterogeneous reactions is fundamentally different from that of the homogeneous reaction catalysed by [IrH<sub>2</sub>(POCOP)] (**1**), which is a dihydride species. The data in Table 1 support such mechanistic difference, as they show different trends for the silica-grafted complex **2** and for its homogeneous counterpart **1** with respect to the different alkene classes. In fact, the heterogeneous catalyst **2** gives the highest hydrogenation rate for 1-decene (the least bulky alkene, TOF = 8.4 h<sup>-1</sup>), followed by a bulky terminal olefin such as 4-phenyl-1-butene (3.8 h<sup>-1</sup>), and finally styrene (2.6 h<sup>-1</sup>), which suggests that steric effects play the major role. The TOF values of cyclohexene, a *cis* cyclic alkene (1.4 h<sup>-1</sup>) and *trans*-5-decene (0.42 h<sup>-1</sup>) support a trend dominated by steric effects with **2**. In contrast, the homogeneous catalyst **1** gives the fastest rate with styrene (18.3 vs. 1.1–0.70 h<sup>-1</sup> for aliphatic alkenes), which suggests that electronic effects are predominant in this case.

In the field of heterogenised catalysts, monohydride mechanisms have been proposed for a number of catalytic systems. Thus, the catalytic alkene hydrogenation with alumina-supported complexes of *f*-elements has been suggested to involve an intermediate alkyl complex that takes part in the heterolytic splitting of coordinated dihydrogen by  $\sigma$ -bond metathesis.<sup>22</sup> The protonation of the alkyl ligand releases the alkane and regenerates the metal-hydride species, as suggested in Scheme 9c.

More recently, a silica-grafted zinc complex has been proposed to hydrogenate propene with the intermediacy of a hydride complex of zinc generated by heterolytic splitting of  $H_2$  with concomitant SiOH formation. The key steps of this mechanism are alkene insertion into the Zn–H bond and the proton transfer from the silanol to release the alkane.<sup>45</sup>

The common features of these three systems are a mechanism based on a constant oxidation state and the occurrence of a  $\sigma$ -bond metathesis involving the alkyl and metal-bound  $H_2$ . Four-center transition states have been widely proposed and represent a well-established reaction pattern at late TM centers.<sup>46</sup> Still, it should be kept in mind that the reaction pathway sketched in Scheme 9 is only a working hypothesis that requires deeper investigation in the future.

## Conclusions

Beside gas-phase reactions, the silica grafted hydride [IrH(O–SBA-15)(POCOP)] (**2**) catalyses the hydrogenation of liquid alkenes when suspended in a suitable solvent under dihydrogen (1 bar). Albeit stable, the silica-grafted complex **2** is intrinsically reactive and requires no activation before catalyzing alkene hydrogenation, which is carried out at room temperature and at atmospheric pressure of dihydrogen. The catalyst was recovered unchanged and reused in catalysis with similar

results. With all alkenes tested (1-decene, *trans*-5-decene, cyclohexene, styrene, and 4-phenyl-1-butene), hot filtration tests showed that the complex does not leach into solution. Also, the silica-grafted hydride of iridium(III) has a smaller tendency to undergo hydrogenolysis of the Ir–siloxo bond, and the reaction is completely suppressed in the presence of propene. Finally, the reactivity pattern of the grafted species **2** differs significantly from that of its soluble dihydride analogue [IrH<sub>2</sub>(POCOP)] (**1**). Overall, although the present work is only the first application of the silica-grafted complex **2** to catalytic reactions in solution, the present results support that silica-grafted complex is the active species in the catalytic hydrogenation and that it resists leaching. With its uniform mononuclear structure, wealth of spectroscopic information, and (in principle) finely tunable catalytic activity, **2** opens new perspectives in the endeavour of closing the gap between homogeneous and heterogeneous catalysis.

## Experimental section

### General

The complexes [IrH<sub>2</sub>(POCOP)] (**1**),<sup>47</sup> [IrH(O–SBA-15)(POCOP)] (**2**),<sup>36</sup> [IrH(OSi<sub>8</sub>O<sub>12</sub>iBu<sub>7</sub>)(POCOP)] (**3**),<sup>37</sup> [IrH(OSiMe<sub>3</sub>)(POCOP)] (**4**),<sup>36</sup> [Ir(C<sub>2</sub>H<sub>4</sub>)(POCOP)] (**6a**),<sup>42</sup> were prepared according to literature procedures.

### Catalytic hydrogenation with [IrH<sub>2</sub>(POCOP)] (**1**)

The homogeneous catalyst [IrH<sub>2</sub>(POCOP)] (**1**) (5 mg, 8.4 μmol) was dissolved in pentane (5 mL) in a 20 mL Young Schlenk tube equipped with a Teflon coated stirring bar under argon. The Schlenk was purged with dihydrogen (1 bar abs.) for 1 min, and the reaction solution was stirred at room temperature for 10 min. The solution colour changed from brown to light yellow, which indicates the formation of the tetrahydride complex [IrH<sub>4</sub>(POCOP)] (**5**). The appropriate amount of alkene (1-decene: 38 μL, 201 μmol; *trans*-5-decene: 38 μL, 201 μmol; cyclohexene 20 μL, 197 μmol; styrene: 23 μL, 201 μmol; 4-phenyl-1-butene: 30 μL, 200 μmol) was added to the stirred reaction mixture by means of a microsyringe through a rubber septum. Samples of the reaction mixture (approximately 0.15 mL) were periodically taken, filtered over silica, and analysed by GC to evaluate the conversion of the alkene into the corresponding alkane (Fig. S3, S12 – S15). The fitting of these approximately linear plots gave the TOF values reported in Table 1. The POSS complex **3** gave similar results with 1-decene (Fig. 2 and S2).

### Catalytic Hydrogenation with [IrH(O–SBA-15)(POCOP)] (**2**)

The silica-grafted catalyst **2** (loading of **1**: 5.6% w/w, 8.4 μmol) was suspended in pentane (5 mL) in a 20 mL-Schlenk tube equipped with a Teflon coated stirring bar under argon. The Schlenk was purged with dihydrogen (1 bar abs.) for 1 minute, and the suspension was stirred at room temperature for 10 min. The appropriate amount of alkene (1-decene: 38 μL, 201 μmol; *trans*-5-decene: 38 μL, 201 μmol; cyclohexene 20 μL, 197 μmol; styrene: 23 μL, 201 μmol; 4-phenyl-1-butene: 30 μL,

200 μmol) was added to the stirred reaction mixture by means of a microsyringe through a rubber septum. Samples of the reaction mixture (approximately 0.15 mL) were periodically taken, filtered over silica, and analysed by GC to determine the conversion of the alkene into the corresponding alkane. During the reaction, the stirring was interrupted and the solid catalyst deposited on the bottom of the Schlenk tube within a few seconds. Most of the supernatant reaction solution was separated by means of a syringe and transferred to a Schlenk tube set under hydrogen (1 bar absolute). Monitoring of reaction progress by GC in the new reaction vessel showed that the concentrations of alkene and alkane remained constant after separation of the solution from the solid catalyst (Fig. S1, S7-S10). The fitting of these approximately linear plots gave the TOF values reported in Table 1.

### Catalytic Hydrogenation with **3**

See Supporting Information.

### Reaction of [IrH(O–SBA-15)(POCOP)] (**2**) with gaseous alkenes

Compound **2** (complex loading of 21% w/w, 38 mg) was placed in a 20 mL-Young Schlenk, the argon atmosphere was replaced with ethene (1.5 bar absolute), and the solid was stirred at room temperature for 6 h. The solid-state <sup>31</sup>P NMR spectrum of the resulting material shows a signal at δ – 182, which is evidence of the formation of the ethene complex [Ir(C<sub>2</sub>H<sub>4</sub>)(POCOP)] (**6a**) (an impurity gives a signal at approximately δ 71). The same procedure was repeated using propene as alkene. Differently from the reaction performed with ethene, the formation of the corresponding iridium(I) propene complex was not observed and was recovered unreacted **2**.

### Reaction of [IrH(O–SBA-15)(POCOP)] (**2**) with alkenes in solution

Compound **2** (approximately 10 – 15 mg with a loading of 13%) was introduced in a Young NMR tube, and [D<sub>8</sub>]toluene (0.6 mL) was added under argon. The alkene was then introduced in the NMR tube. The addition of gaseous alkenes (propene or ethene) was performed evacuating the NMR tube and introducing then 1.4 bar (abs.) of the gaseous alkene. Alternatively, the liquid alkene (1-dodecene, approximately 20 μL) was introduced in the NMR tube under argon with a microsyringe. After the addition of the alkene, the tube was shaken to mix the reagents, and the solid was deposited on the bottom by centrifugation prior to measurement. The <sup>31</sup>P and <sup>1</sup>H NMR spectra were recorded to analyse the soluble species. The reaction with ethene gave a new species in solution, the complex [Ir(C<sub>2</sub>H<sub>4</sub>)(POCOP)] (**6a**), identified by the <sup>31</sup>P NMR chemical shift at δ 180.6 and the <sup>1</sup>H NMR shift of the coordinated ethene ligand at δ 3.05. No dissolved species were observed with all other alkenes.

### Reaction of [IrH(OSi<sub>8</sub>O<sub>12</sub>iBu<sub>7</sub>)(POCOP)] (**3**) with alkenes

Complex **3** (10 mg) was introduced in a Young NMR tube and then dissolved in [D<sub>10</sub>]p-xylene under argon. The argon atmosphere was replaced with ethene (1 bar abs.), and the progress of the reaction was monitored by NMR spectroscopy.

Just after the addition of ethene, the  $^{31}\text{P}$  NMR spectrum showed only the presence of the starting material **3** (singlet at  $\delta$  170.2). After 2.3 h, a signal corresponding to  $[\text{Ir}(\text{C}_2\text{H}_4)(\text{POCOP})]$  (**6a**) appeared (singlet at  $\delta$  180.6, 6 %). A conversion of 84 % was observed after 29.8 h. With propene or 1-dodecene as alkenes, the  $^{31}\text{P}$  NMR spectra of the reaction solution showed exclusively the signal of unreacted **3** even after 24 h.

#### Reaction of $[\text{IrH}(\text{OSiMe}_3)(\text{POCOP})]$ (**4**) with ethene

Complex **4** (34 mg, 0.06 mmol) was dissolved in  $[\text{D}_{10}]p$ -xylene (1 mL) in a 20 mL-Young Schlenk tube under argon. The argon atmosphere was replaced with ethene (1.5 bar absolute), and the solution was stirred for 1 h. The  $^1\text{H}$  and  $^{31}\text{P}$  NMR spectra indicated the formation of the ethene complex **6a**. Crystals suitable for X-ray were obtained from the solution and the structure of **6a** was thus solved.

#### Reaction of $[\text{Ir}(\text{C}_2\text{H}_4)(\text{POCOP})]$ (**6a**) with SBA-15

$[\text{Ir}(\text{C}_2\text{H}_4)(\text{POCOP})]$  (**6a**) (6 mg, 9.7  $\mu\text{mol}$ ) and SBA-15 (97 mg) were introduced in a 20 mL Young Schlenk tube and then pentane (4 mL) was added under argon. The resulting mixture was stirred at room temperature for 50 min. The solvent is removed in vacuum and the resulting solid (87 mg) dried in vacuum for 2 h. The  $^{31}\text{P}$  solid-state MAS NMR spectrum of the reaction product show the formation of the species  $[\text{IrH}(\text{O}-\text{SBA-15})(\text{POCOP})]$  (**2**) ( $\delta$  171) along with unreacted **6a** ( $\delta$  182).

#### Reaction of $[\text{Ir}(\text{C}_3\text{H}_6)(\text{POCOP})]$ (**6b**) with SBA-15

$[\text{Ir}(\text{C}_3\text{H}_6)(\text{POCOP})]$  (**6b**) (5.5 mg, 8.7  $\mu\text{mol}$ ) and SBA-15 (95 mg) were introduced in a 20 mL Young Schlenk tube and then pentane (4 mL) was added under argon. The resulting mixture was stirred at room temperature for 50 min. The solvent is removed in vacuum and the resulting solid dried in vacuum for 2 h. The  $^{31}\text{P}$  solid-state MAS NMR spectrum of the reaction product show the exclusive formation of the species  $[\text{IrH}(\text{O}-\text{SBA-15})(\text{POCOP})]$  (**2**) ( $\delta$  171).

#### Reaction of $[\text{Ir}(\text{C}_2\text{H}_4)(\text{POCOP})]$ (**6a**) with *i*Bu-POSS-OH

The complex  $[\text{Ir}(\text{C}_2\text{H}_4)(\text{POCOP})]$  (**6a**) (18.9 mg, 31  $\mu\text{mol}$ ) and *i*Bu-POSS-OH (51 mg, 61  $\mu\text{mol}$ ) were dissolved in  $[\text{D}_8]$ toluene (0.6 mL) in a Young NMR tube under argon. The  $^{31}\text{P}$  and  $^1\text{H}$  NMR spectra of the reaction solution showed no formation of new products after some hours. Alternatively the reaction was performed in a 20 mL-Young Schlenk tube. In a typical procedure,  $[\text{Ir}(\text{C}_2\text{H}_4)(\text{POCOP})]$  (**6a**) (18.2 mg, 29  $\mu\text{mol}$ ) and *i*Bu-POSS-OH (54 mg, 65  $\mu\text{mol}$ ) were dissolved in  $[\text{D}_8]$ toluene (1 mL) under argon, and the resulting solution was heated at 80 °C under static vacuum. After 2 h, the  $^{31}\text{P}$  and  $^1\text{H}$  NMR spectra of the reaction mixture showed the formation of  $[\text{IrH}(\text{OSi}_8\text{O}_{12}i\text{Bu}_7)(\text{POCOP})]$  (**3**) (14%). Upon additional 10 h of heating at 80 °C under static vacuum, the yield of  $[\text{IrH}(\text{OSi}_8\text{O}_{12}i\text{Bu}_7)(\text{POCOP})]$  (**3**) reached 29% (based on the integration of the  $^{31}\text{P}$  NMR spectrum).

#### Reaction of $[\text{Ir}(\text{C}_3\text{H}_6)(\text{POCOP})]$ (**6b**) with *i*Bu-POSS-OH

The complex  $[\text{Ir}(\text{C}_3\text{H}_6)(\text{POCOP})]$  (**6b**) (7.0 mg, 11  $\mu\text{mol}$ ) and *i*Bu-POSS-OH (21 mg, 25  $\mu\text{mol}$ ) were dissolved in  $[\text{D}_8]$ toluene (0.8 mL) in a Young NMR tube under argon. After 10 min, the  $^{31}\text{P}$  and  $^1\text{H}$  NMR spectra of the reaction solution showed 22% conversion to the product  $[\text{IrH}(\text{OSi}_8\text{O}_{12}i\text{Bu}_7)(\text{POCOP})]$  (**3**) ( $^{31}\text{P}$  NMR shift at  $\delta$  170.5). Alternatively, the reaction was performed in a 20 mL-Young Schlenk tube. In a typical procedure,  $[\text{Ir}(\text{C}_3\text{H}_6)(\text{POCOP})]$  (**6b**) (6.5 mg, 10  $\mu\text{mol}$ ) and *i*Bu-POSS-OH (21 mg, 25  $\mu\text{mol}$ ) were dissolved in  $[\text{D}_8]$ toluene (0.8 mL) under argon, and the resulting solution was heated at 80 °C under static vacuum for two hours. The  $^{31}\text{P}$  and  $^1\text{H}$  NMR spectra showed complete conversion to  $[\text{IrH}(\text{OSi}_8\text{O}_{12}i\text{Bu}_7)(\text{POCOP})]$  (**3**).

#### Reaction of $[\text{IrH}(\text{O}-\text{SBA-15})(\text{POCOP})]$ (**2**) with dihydrogen

Complex **2** (10 mg, 5.6% w/w loading) was suspended in deuterated toluene (0.6 mL) in a Young NMR tube under argon. The argon atmosphere was replaced with dihydrogen (1 bar abs.), the tube was shaken several times, and the solid was deposited on the bottom of the tube by centrifugation. The  $^1\text{H}$  NMR spectrum of the solution recorded immediately thereafter showed a very weak signal at  $\delta$  - 8.4, corresponding to the tetrahydride complex  $[\text{IrH}_4(\text{POCOP})]$  (**5**) whose intensity remained constant over 30 min. Although hardly detectable, the tetrahydride complex **5** was quantified to be approximately 4% of the initial complex loading by using trimethylbenzene as internal standard. When the same test was performed under a dihydrogen/propene atmosphere (1:1, 2 bar absolute), the signal of **5** was not detected by  $^1\text{H}$  NMR spectroscopy over 45 min.

#### Reaction of $[\text{IrH}(\text{OSi}_8\text{O}_{12}i\text{Bu}_7)(\text{POCOP})]$ (**3**) with dihydrogen

Complex **3** (12 mg, 8.4  $\mu\text{mol}$ ) was dissolved in pentane (5 mL) in a Schlenk tube (20 mL) under argon. After purging with dihydrogen (1 bar abs.) for 1 minute and stirring at room temperature for 10 min, the colour of the catalyst solution changed from red to light yellow. The  $^{31}\text{P}$  NMR spectrum of a sample thereof indicated the presence in solution of a mixture of  $[\text{IrH}_2(\text{POCOP})]$  (**1**) (singlet at  $\delta$  203.0, 42 %),  $[\text{IrH}_4(\text{POCOP})]$  (**5**) (singlet at  $\delta$  181.7, 38 %), and  $[\text{IrH}(\text{OSi}_8\text{O}_{12}i\text{Bu}_7)(\text{POCOP})]$  (**3**) (singlet at  $\delta$  170.0, 19 %). Then, 1-decene (38  $\mu\text{L}$ , 201  $\mu\text{mol}$ ) was introduced by means of a microsyringe through a rubber septum. The reaction solution became red within few seconds, and its  $^{31}\text{P}$  NMR spectrum showed the presence of the alkene complex  $[\text{Ir}(\text{C}_{10}\text{H}_{20})(\text{POCOP})]$  ( $\delta$  179.0) as the only product.

#### Synthesis of $[\text{Ir}(\text{C}_3\text{H}_6)(\text{POCOP})]$ (**6b**)

Complex **1** (26 mg, 44  $\mu\text{mol}$ ) was dissolved in hexane (4 mL) in a 20 mL-Young Schlenk. The argon atmosphere was replaced with propyne (1.5 bar abs.), and the resulting solution was stirred for 30 min. A red solid was obtained by evaporating the solvent in vacuum. Red crystals suitable for X-ray were obtained by slow evaporation of a toluene solution.  $^1\text{H}$  NMR (500 MHz,  $[\text{D}_{10}]p$ -xylene, RT)  $\delta$  = 7.10 (m, 2H; arom), 6.93 (m, 1H; arom), 4.68 (m, 1H;  $\text{CH}_2\text{CHCH}_3$ ), 3.95 (d,  $J$  = 9.9 Hz, 1H;  $\text{CH}_2\text{CHCH}_3$ ), 2.62 (d,  $J$  = 8.1 Hz, 1H;  $\text{CH}_2\text{CHCH}_3$ ), 1.86 (d,  $J$  = 5.9 Hz, 3H;  $\text{CH}_2\text{CHCH}_3$ ), 1.53 (s, 18H;  $\text{C}(\text{CH}_3)_3$ ), 1.36 (s, 18H;  $\text{C}(\text{CH}_3)_3$ );  $^{31}\text{P}$  NMR (202 MHz,  $[\text{D}_{10}]p$ -xylene, RT):  $\delta$  = 180.4 (s);

$^{13}\text{C}$  NMR (125 MHz,  $[\text{D}_{10}]\rho$ -xylene, RT):  $\delta$  = 168.5 (t,  $J$  = 8.2 Hz, 2C;  $\text{C}_q$  C–O), 143.1 (t,  $J$  = 8.6 Hz, 1C; arom), 127.5 (m, 1C; CH arom), 104.5 (m, 2C; CH arom), 46.0 (s, 1C;  $\text{CH}_2\text{CHCH}_3$ ), 43.4 (t,  $J$  = 11.2 Hz, 2C;  $\text{C}_q$  C( $\text{CH}_3$ ) $_3$ ), 42.8 (t,  $J$  = 11.0 Hz, 2C;  $\text{C}_q$  C( $\text{CH}_3$ ) $_3$ ), 41.2 (s,  $\text{CH}_2\text{CHCH}_3$ ), 30.3 (t,  $J$  = 2.8 Hz, 6C; C( $\text{CH}_3$ ) $_3$ ), 29.3 (t,  $J$  = 2.9 Hz, 6C; C( $\text{CH}_3$ ) $_3$ ), 22.5 (s, 1C;  $\text{CH}_2\text{CHCH}_3$ ); elemental analysis calcd (%) for  $\text{C}_{25}\text{H}_{45}\text{IrO}_2\text{P}_2$ : C 47.53, H 7.18; found: C 47.72, H 7.24.

### Synthesis of $[\text{Ir}(\text{C}_{10}\text{H}_{20})(\text{POCOP})]$ (**6c**)

Complex **1** (26.4 mg, 44.6  $\mu\text{mol}$ ) was dissolved in pentane (2 mL) in a 20 mL-Young Schlenk under argon. Upon adding 1-decene (18  $\mu\text{L}$ ), the solution changed colour from brown to red. After stirring at room temperature for 1 h, removing the volatiles under vacuum gave a red solid.  $^1\text{H}$  NMR (500 MHz,  $[\text{D}_{10}]\rho$ -xylene, RT):  $\delta$  = 7.1 (t,  $J$  = 7.8 Hz, 1H; arom.), 6.94 (d,  $J$  = 7.9 Hz, 2H; arom.), 4.73 (br m, 1H;  $\text{CH}_2\text{CHCH}_2$ –), 4.00 (m, 1H;  $\text{CH}_2\text{CHCH}_2$ –), 2.66 (d,  $J$  = 8.0 Hz, 1H;  $\text{CH}_2\text{CHCH}_2$ –), 2.43 (br m, 1H), 1.77 (br m, 2H), 1.70 – 1.43 (br m, 11H), 1.56 (t,  $J$  = 6.5 Hz, 18H; C( $\text{CH}_3$ ) $_3$ ), 1.40 (t,  $J$  = 6.6 Hz, 18H; C( $\text{CH}_3$ ) $_3$ ), 1.11 ppm (t,  $J$  = 6.7 Hz, 3H;  $-\text{CH}_2\text{CH}_3$ );  $^{31}\text{P}$  NMR (202 MHz,  $[\text{D}_{10}]\rho$ -xylene, RT):  $\delta$  = 179.6 ppm (s);  $^{13}\text{C}$  NMR (125 MHz,  $[\text{D}_{10}]\rho$ -xylene, RT):  $\delta$  = 168.6 (t,  $J$  = 8.5 Hz, 2C;  $\text{C}_q$  C–O), 143.6 (t,  $J$  = 8.7 Hz, 1C; arom), 127.7 (s, 1C; CH arom), 104.5 (t,  $J$  = 5.9 Hz, 2C; CH arom), 52.7 (s, 1C;  $\text{CH}_2\text{CHCH}_2$ –), 43.5 (t,  $J$  = 11.2 Hz, 2C;  $\text{C}_q$  C( $\text{CH}_3$ ) $_3$ ), 42.8 (t,  $J$  = 10.8 Hz, 2C;  $\text{C}_q$  C( $\text{CH}_3$ ) $_3$ ), 40.3 (s, 1C;  $\text{CH}_2\text{CHCH}_2$ –), 38.2 (s, 1C;  $\text{CH}_2$ ), 35.3 (s, 1C;  $\text{CH}_2$ ), 33.5 (s, 1C;  $\text{CH}_2$ ), 31.1 (s, 1C;  $\text{CH}_2$ ), 30.9 (s, 1C;  $\text{CH}_2$ ), 30.9 (s, 1C;  $\text{CH}_2$ ), 30.3 (t,  $J$  = 2.3 Hz, 6C; C( $\text{CH}_3$ ) $_3$ ), 29.3 (t,  $J$  = 2.6 Hz, 6C; C( $\text{CH}_3$ ) $_3$ ), 24.2 (s, 1C;  $\text{CH}_2$ ), 15.3 (s, 1C;  $-\text{CH}_2\text{CH}_3$ ); elemental analysis calcd (%) for  $\text{C}_{32}\text{H}_{59}\text{IrO}_2\text{P}_2$ : C 52.65, H 8.15; found: C 52.59, H 8.07.

### Notes and references

‡ Worth of note is the value of the intercept at 8.33, that indicates a virtual 1-decene conversion of 8.3% at time zero. This fact, in addition to the appearance of an orange-red colour of the solution upon addition of the substrate (1-decene) and its persistence during the catalysis, speaks in favour of the predominant formation of the alkene complex  $[\text{Ir}(\text{alkene})(\text{POCOP})]$ , instead of the di/tetrahydride complex. Therefore, considering the catalyst loading and that under hydrogen atmosphere the tetrahydride complex  $[\text{IrH}_4(\text{POCOP})]$  (**5**) is formed, a conversion of 8.25% can be calculated as result of the effect of the dihydrogen already coordinated to the metal center as tetrahydride complex. The value of 8.3 % conversion is well in agreement with the calculated one and is consistent with a rapid formation of the alkene complex, which hydrogenates the alkene at a lower rate than **5**.

§ In a control experiment, SBA-15 resulted inactive in 1-decene isomerisation.

¶ Details of the crystallographic analyses are given in the Supporting Information. CCDC 988733 (**6a**) and 988734 (**6b**) contain the supplementary crystallographic data for this paper. These data can be obtained free of charge from The Cambridge Crystallographic Data Centre via [www.ccdc.cam.ac.uk/data\\_request/cif](http://www.ccdc.cam.ac.uk/data_request/cif).

|| In the hydrogenation of liquid alkenes with the soluble dihydride complex **1**, the iridium(I) alkene complex is the only species detected in solution by  $^{31}\text{P}$  NMR spectroscopy after the initial hydrogenation activity given by the tetrahydride complex **5** (see also footnote ‡).

- 1 J. M. Basset, R. Psaro, D. Roberto and R. Ugo, *Modern Surface Organometallic Chemistry*, Wiley-VCH, Weinheim, 2009.
- 2 J. M. Thomas, *Design and Application of Single-Site Heterogeneous Catalysts*, Imperial College Press, London, 2012.

- 3 J. M. Thomas, *J. Chem. Phys.*, 2008, **128**, 182502 - 182518.
- 4 J. M. Thomas, R. Raja and D. W. Lewis, *Angew. Chem. Int. Ed.*, 2005, **44**, 6456-6482.
- 5 R. Anwender, *Chem. Mater.*, 2001, **13**, 4419-4438.
- 6 R. Buffon and R. Rinaldi, in *Modern Surface Organometallic Chemistry*, eds. J. M. Basset, R. Psaro, D. Roberto and R. Ugo, Wiley-VCH, Weinheim, 2009, pp. 417-453.
- 7 T. Maschmeyer, F. Rey, G. Sankar and J. M. Thomas, *Nature*, 1995, **378**, 159-162.
- 8 J. Corker, F. Lefebvre, C. Léculuyer, V. Dufaud, F. Quignard, A. Choplin, J. Evans and J.-M. Basset, *Science*, 1996, **271**, 966-969.
- 9 V. Vidal, A. Théolier, J. Thivolle-Cazat and J.-M. Basset, *Science*, 1997, **276**, 99-102.
- 10 G. G. Hlatky, *Chem. Rev.*, 2000, **100**, 1347-1376.
- 11 J. Jarupatrakorn and T. D. Tilley, *J. Am. Chem. Soc.*, 2002, **124**, 8380-8388.
- 12 C. P. Nicholas, H. Ahn and T. J. Marks, *J. Am. Chem. Soc.*, 2003, **125**, 4325-4331.
- 13 L. A. Williams and T. J. Marks, *ACS Catal.*, 2011, **1**, 238-245.
- 14 C. Tiozzo, C. Bisio, F. Carniato, A. Gallo, S. L. Scott, R. Psaro and M. Guidotti, *PCCP*, 2013, **15**, 13354-13362.
- 15 J. M. Thomas, *PCCP*, 2014, **16**, 7647-7661.
- 16 D. G. H. Ballard, in *Advances in Catalysis*, eds. H. P. D.D. Eley and B. W. Paul, Academic Press, 1973, pp. 263-325.
- 17 V. A. Zakharov, V. K. Dudchenko, E. A. Paukshtis, L. G. Karakchiev and Y. I. Yermakov, *J. Mol. Catal.*, 1977, **2**, 421-435.
- 18 J. Schwartz and M. D. Ward, *J. Mol. Catal.*, 1980, **8**, 465-469.
- 19 Y. I. Yermakov, Y. A. Ryndin, O. S. Alekseev, D. I. Kochubey, V. A. Shmachkov and N. I. Gergert, *J. Mol. Catal.*, 1989, **49**, 121-132.
- 20 V. A. Zakharov and Y. A. Ryndin, *J. Mol. Catal.*, 1989, **56**, 183-193.
- 21 R. G. Bowman, R. Nakamura, P. J. Fagan, R. L. Burwell and T. J. Marks, *J. Chem. Soc., Chem. Commun.*, 1981, 257-258.
- 22 T. J. Marks, *Acc. Chem. Res.*, 1992, **25**, 57-65.
- 23 M. Y. He, G. Xiong, P. J. Toscano, R. L. Burwell and T. J. Marks, *J. Am. Chem. Soc.*, 1985, **107**, 641-652.
- 24 W. C. Finch, R. D. Gillespie, D. Hedden and T. J. Marks, *J. Am. Chem. Soc.*, 1990, **112**, 6221-6232.
- 25 R. D. Gillespie, R. L. Burwell and T. J. Marks, *Langmuir*, 1990, **6**, 1465-1477.
- 26 M. S. Eisen and T. J. Marks, *J. Am. Chem. Soc.*, 1992, **114**, 10358-10368.
- 27 M. K. Richmond, S. L. Scott and H. Alper, *J. Am. Chem. Soc.*, 2001, **123**, 10521-10525.
- 28 C. Nozaki, C. G. Lugmair, A. T. Bell and T. D. Tilley, *J. Am. Chem. Soc.*, 2002, **124**, 13194-13203.
- 29 M. Tada, T. Sasaki and Y. Iwasawa, *PCCP*, 2002, **4**, 4561-4574.
- 30 R. L. Brutchey, I. J. Drake, A. T. Bell and T. D. Tilley, *Chem. Commun.*, 2005, 3736-3738.
- 31 B. Marciniak, K. Szubert, M. J. Potrzebowski, I. Kownacki and K. Łęszczak, *Angew. Chem. Int. Ed.*, 2008, **47**, 541-544.
- 32 Y. S. Choi, E. G. Moschetta, J. T. Miller, M. Fasulo, M. J. McMurdo, R. M. Rioux and T. D. Tilley, *ACS Catal.*, 2011, **1**, 1166-1177.
- 33 M. Rimoldi and A. Mezzetti, *Catal. Sci. Technol.*, 2014, **4**, 2724.
- 34 H. C. Foley, S. J. DeCanio, K. D. Tau, K. J. Chao, J. H. Onuferko, C. Dybowski and B. C. Gates, *J. Am. Chem. Soc.*, 1983, **105**, 3074-3082.
- 35 J. Lu, C. Aydin, N. D. Browning and B. C. Gates, *J. Am. Chem. Soc.*, 2012, **134**, 5022-5025.
- 36 M. Rimoldi, D. Fodor, J. A. van Bokhoven and A. Mezzetti, *Chem. Commun.*, 2013, **49**, 11314-11316.
- 37 M. Rimoldi and A. Mezzetti, *Inorg. Chem.*, 2014, **53**, 11974-11984.

## ARTICLE

## Catalysis Science &amp; Technology

- 38 S. Biswas, Z. Huang, Y. Choliy, D. Y. Wang, M. Brookhart, K. Krogh-Jespersen and A. S. Goldman, *J. Am. Chem. Soc.*, 2012, **134**, 13276-13295.
- 39 D. S. Cunha and G. M. Cruz, *Appl. Catal., A*, 2002, **236**, 55-66.
- 40 M. L. M. Bonati, T. M. Douglas, S. Gaemers and N. Guo, *Organometallics*, 2012, **31**, 5243-5251.
- 41 Z. Huang, P. S. White and M. Brookhart, *Nature*, 2010, **465**, 598-601.
- 42 A. S. Goldman, A. H. Roy, Z. Huang, R. Ahuja, W. Schinski and M. Brookhart, *Science*, 2006, **312**, 257-261.
- 43 A. C. Sykes, P. White and M. Brookhart, *Organometallics*, 2006, **25**, 1664-1675.
- 44 Y. Fan, X. Cui, K. Burgess and M. B. Hall, *J. Am. Chem. Soc.*, 2004, **126**, 16688-16689.
- 45 N. M. Schweitzer, B. Hu, U. Das, H. Kim, J. Greeley, L. A. Curtiss, P. C. Stair, J. T. Miller and A. S. Hock, *ACS Catal.*, 2014, 1091-1098.
- 46 R. N. Perutz and S. Sabo-Etienne, *Angew. Chem. Int. Ed.*, 2007, **46**, 2578-2592.
- 47 I. Gottker-Schnetmann, P. S. White and M. Brookhart, *Organometallics*, 2004, **23**, 1766-1776.